

Modélisation numérique de la sismicité induite par la stimulation hydraulique des réservoirs géothermiques

Frederic L. PELLET, Dac T. NGO, Dominique BRUEL

MINES ParisTech - PSL Research University - France

Geotref

Plate-forme pluridisciplinaire d'innovation et de démonstration pour l'exploration et le développement de la **GEOThermie haute énergie dans les REservoirs Fracturés**



Améliorer la compréhension du fonctionnement des réservoirs géothermiques fracturés :

En phase d'exploration : maîtriser le risque lié aux investissements importants pour la réalisation de forages sans avoir la certitude de mettre en évidence une ressource géothermique économiquement exploitable,

En phase de production : garantir une exploitation durable du réservoir.

... et avec le soutien de



Outlines

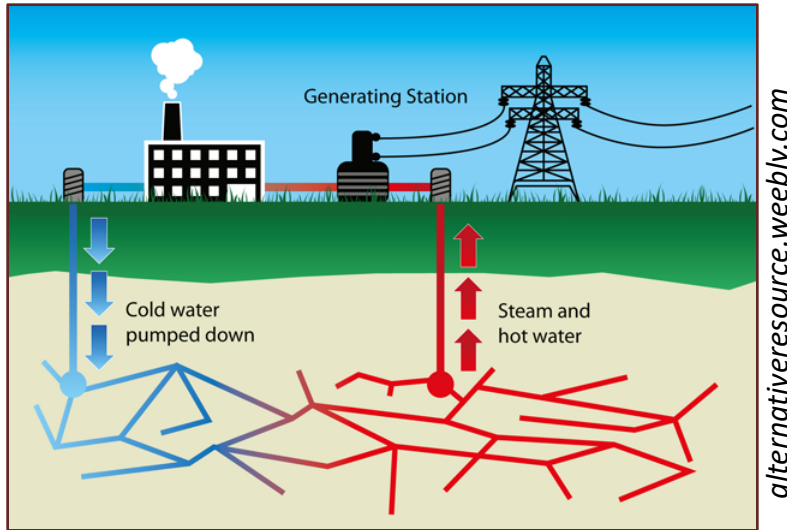
- **Introduction to deep geothermal system**
- **Simulation scenarii and theoretical background**
- **Fracture propagation and fault slip due to hydraulic stimulation ***
- **Induced dynamic effects and wave propagation**
- **Conclusions**

* Ngo, D.T. et al. (2019), Modeling of fault slip during hydraulic stimulation in a naturally fractured medium, Geomechanics and Geophysics for Geo-Energy and Georesources, *In Press*

Introduction to deep geothermal system

Introduction to deep geothermal systems

Reservoirs characteristics: Few km in depth, Mostly in igneous rocks



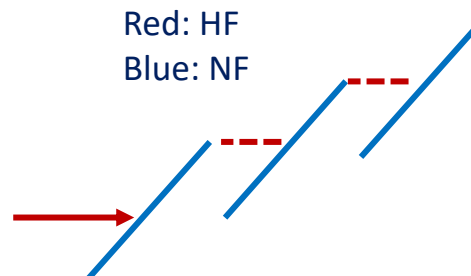
Required properties for an EGS reservoir
(Rybach, 2010)

Property	Value
Fluid production rate	50 – 100 L/s
Wellhead temperature	150 – 200 °C
Total effective heat exchange surface	> 2 x 10 ⁶ m ²
Rock volume	> 2 x 10 ⁸ m ³
Flow impedance	< 0.1 MPa/(L/s)
Water loss	< 10%

Fluid circulation over 20 to 30 years

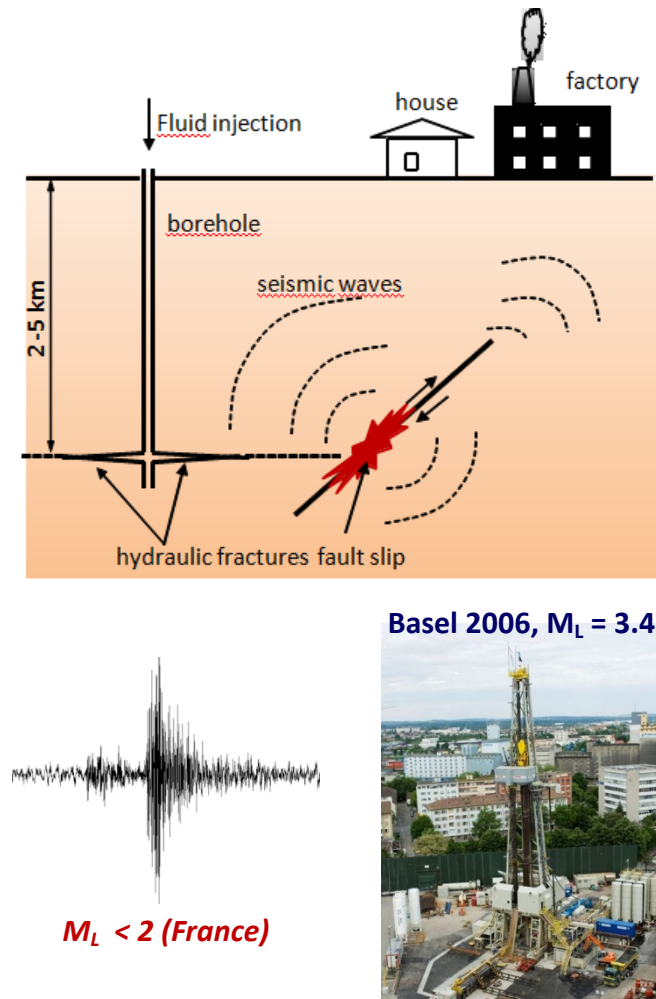
Create a large exchange surface

→ Hydraulic stimulation



Introduction to Deep Geothermal Systems

Associated Risks: Fault Reactivation - Induced Seismicity



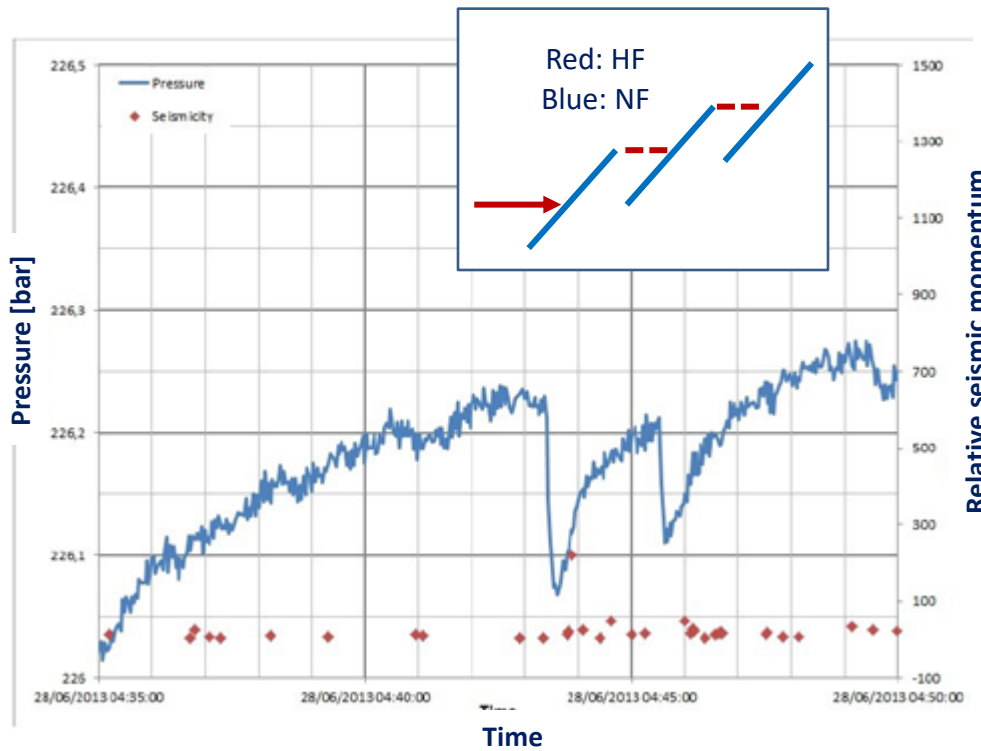
Modified Mercali intensity scale and corresponding peak ground acceleration and peak ground velocity

Source: (Wald et al., 1999; Wood and Neumann, 1931)

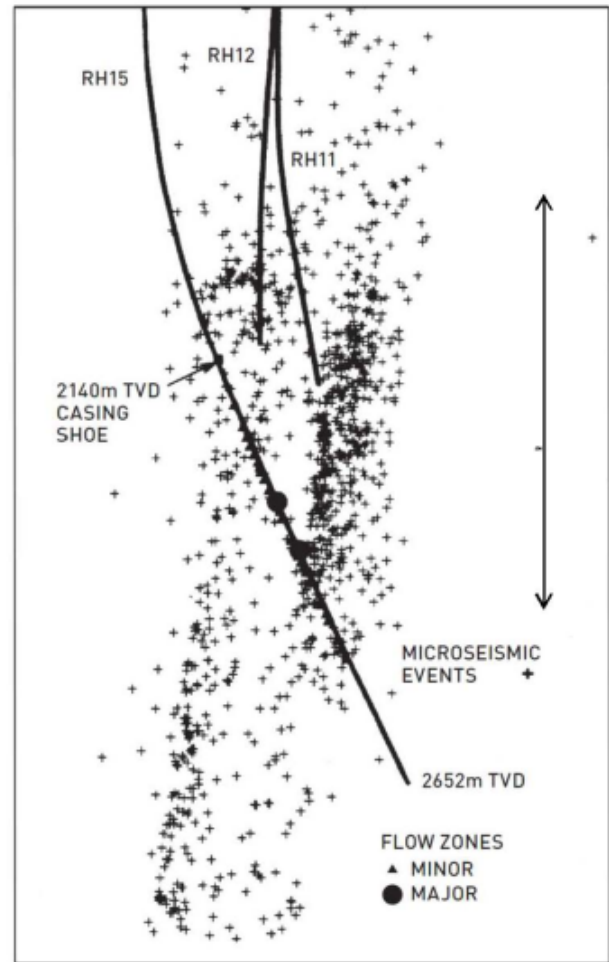
Intensity	Peak acceleration (% g)	Peak velocity (cm/s)	Perceived shaking	Potential damage
I	< 0.17	< 0.1	Not felt	None
II–III	0.17–1.4	0.1–1.1	Weak	None
IV	1.4–3.9	1.1–3.4	Light	None
V	3.9–9.2	3.4–8.1	Moderate	Very light
VI	9.2–18	8.1–16	Strong	Light
VII	18–34	16–31	Very strong	Moderate
VIII	34–65	31–60	Severe	Moderate to heavy
IX	65–124	60–116	Violent	Heavy
X+	> 124	> 116	Extreme	Very heavy

Introduction to Deep Geothermal Systems

Examples of induced seismicity in EGS



Pressure drops and their associated burst of seismicity
at Rittershoffen (Meyer et al, 2017)

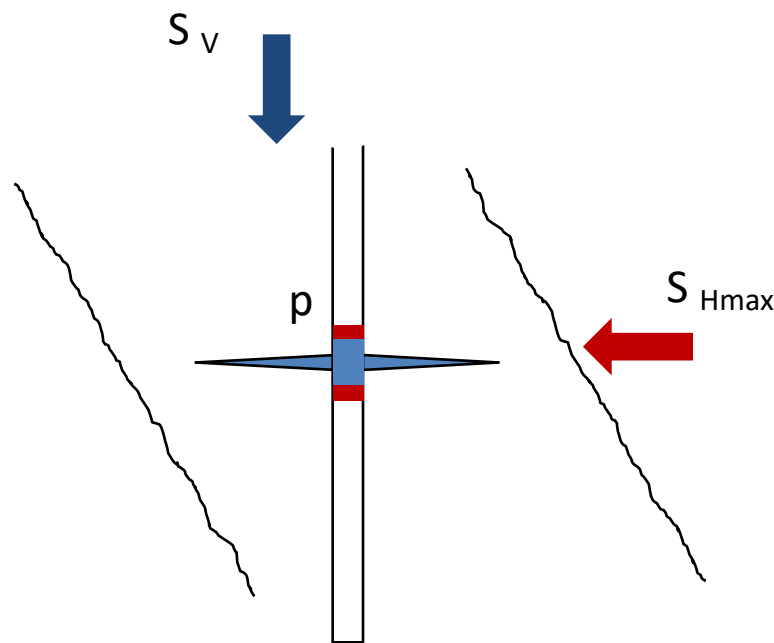


Front view of the seismic cloud of the EGS-
system at Rosemanowes (Parker, 1989)

Simulation scenarii and theoretical background

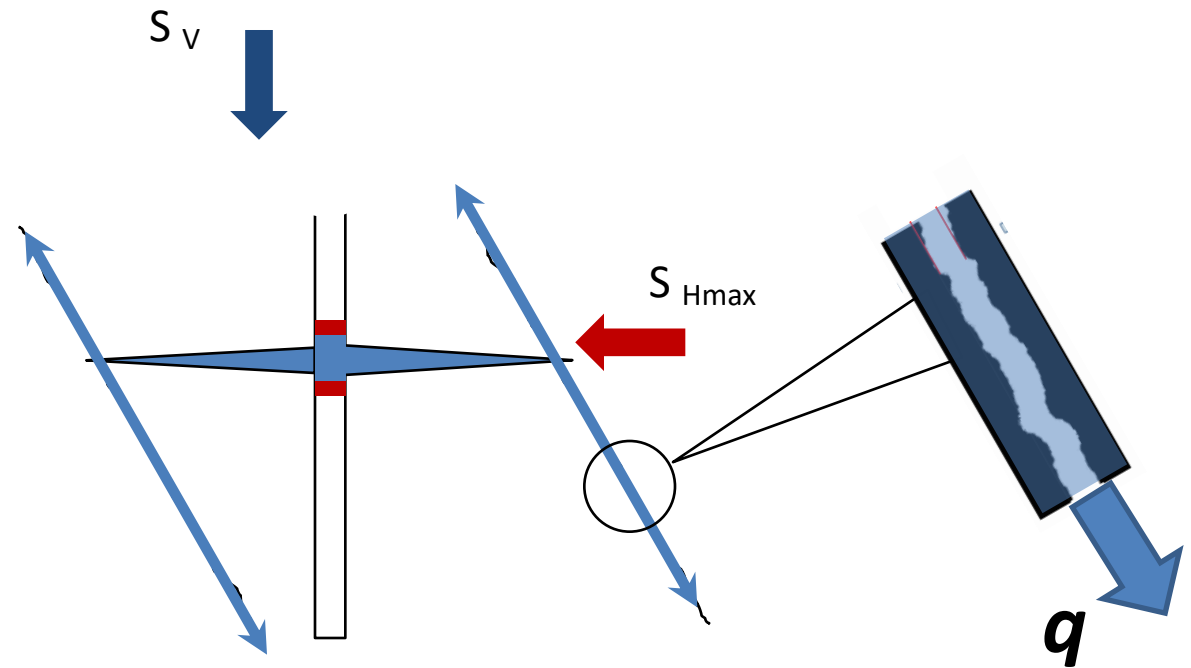
Sequences of hydraulic stimulation

Fracture initiation and propagation



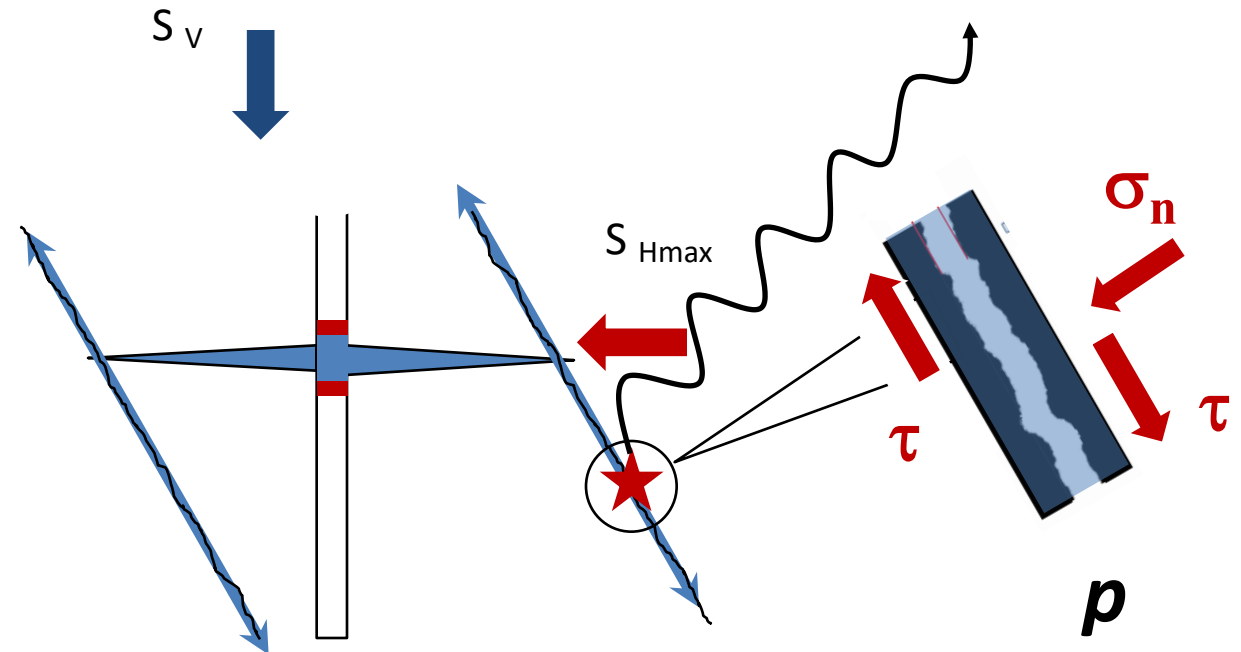
Sequences of hydraulic stimulation

Connection to Fracture Networks: Hydraulics Flow



Sequences of hydraulic stimulation

Fault reactivation and seismic waves



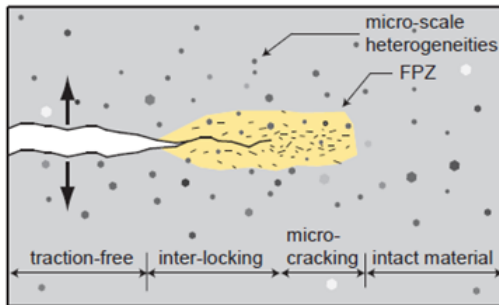
Numerical Simulation Technique

- Initiation and propagation of new fractures
- Deformation of the porous rock mass
- Flow of the fluid within the fractures
- Flow of the fluid within the pores
- Reactivation of existing faults
- Seismic wave propagation
- ~~Heat transfer~~

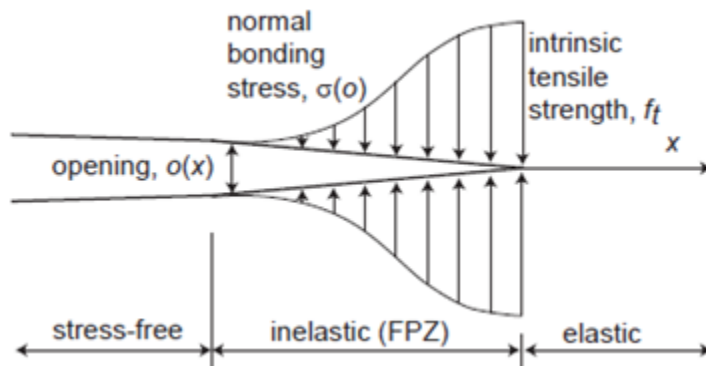
Finite Element Analysis (Abaqus)

Theoretical Background

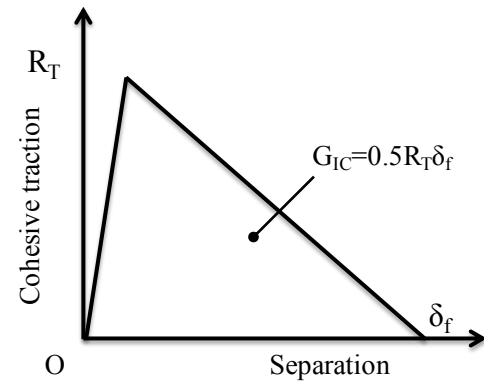
Initiation and propagation of new fracture (Mode I)



after Labuz et al. (1985), modified by Lisjak-Bradley (2013)



Cohesive material concept
(Hillerborg, 1976)



Fracture initiation criterion:

$$\sigma'_{max} = R_T$$

G_{lc} : Energy release rate

Theoretical Background

Deformation of porous rock (thermal effect ignored)

$$\sigma_{ij} - \sigma_{ij}^0 = \left(K - \frac{2}{3}G \right) \varepsilon_V \delta_{ij} + 2G\varepsilon_{ij} - b(p - p_0)\delta_{ij}$$

$$\sigma'_{ij} - \sigma'^0_{ij} = \left(K - \frac{2}{3}G \right) \varepsilon_V \delta_{ij} + 2G\varepsilon_{ij}$$

- K and G are the bulk modulus and the shear modulus of the skeleton

$$\sigma'_{ij} = \sigma_{ij} - bp\delta_{ij}$$

$$b = 1 - \frac{K}{K_s}$$

- b is the Biot's coefficient, which is related to the bulk modulus K of the skeleton and the bulk modulus K_s of the solid phase

$$\nabla \cdot \sigma_{ij} = 0$$

Theoretical Background

Fluid flow within hydraulic fractures and faults

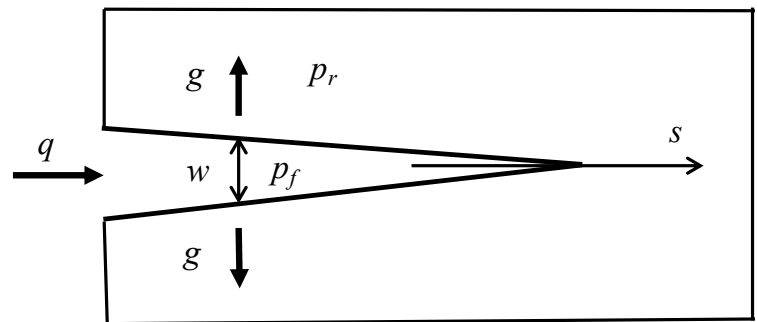
$$\frac{\partial w}{\partial t} + \frac{\partial q}{\partial s} + g = 0$$

$$g(\mathbf{x}, t) = \frac{2C_L}{\sqrt{t - t_0}}$$

$$q = -\frac{w^3}{12\eta} \frac{\partial p}{\partial s}$$
 Poiseuille eq.

$$k_t = \frac{w^3}{12\eta}$$
 Transmissivity

$$\frac{\partial w}{\partial t} - \frac{\partial}{\partial s} \left(\frac{w^3}{12\eta} \frac{\partial p}{\partial s} \right) + g = 0$$



$g(\mathbf{x}, t)$ Infiltration rate from both faces of the hydraulic fracture

C_L Carter's leak off coefficient

η Dynamic viscosity of the fluid

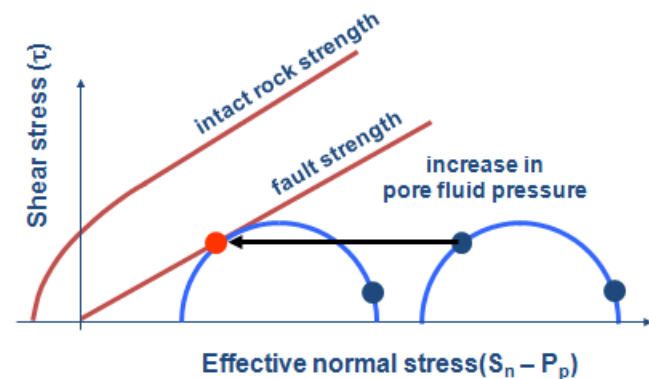
Theoretical Background

Reactivation of critically stress faults

$$R_s = \mu \sigma'_n$$

Coulomb friction law

Others models: stick slip, rate and state



Seismic wave propagation

$$\nabla \cdot \sigma + \rho g = \rho \frac{\partial^2 u}{\partial t^2}$$

$$C_p = \sqrt{\frac{E}{\rho}} \quad C_s = \sqrt{\frac{G}{\rho}}$$

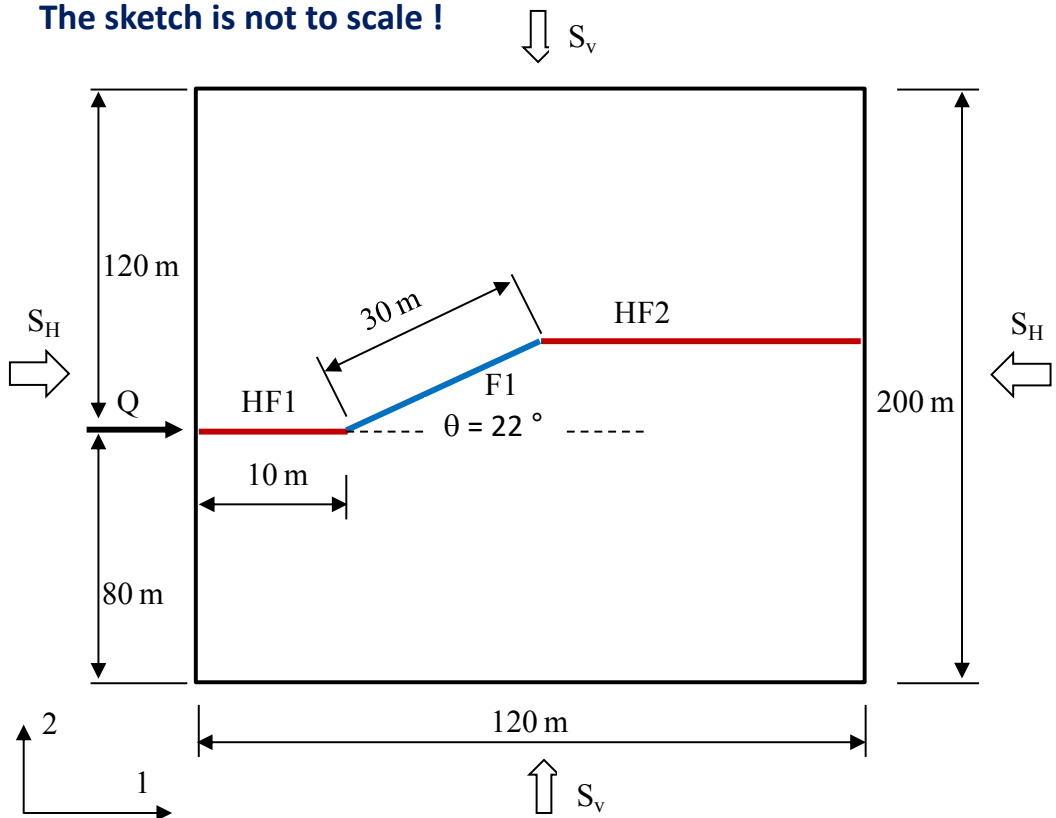
Simulation of fracture propagation and fault slip due to hydraulic stimulation

Slip induced by injection in a single fault model

After Atkinson 1989, Keshavarz 2009, Meyer 2017

2D coupled stress-transient diffusion

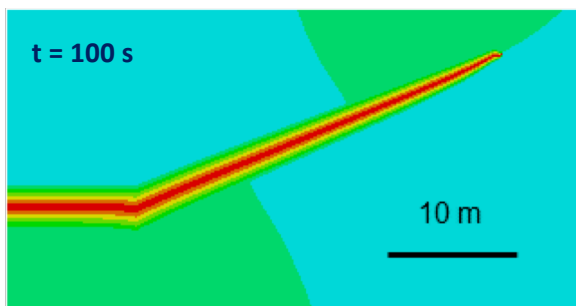
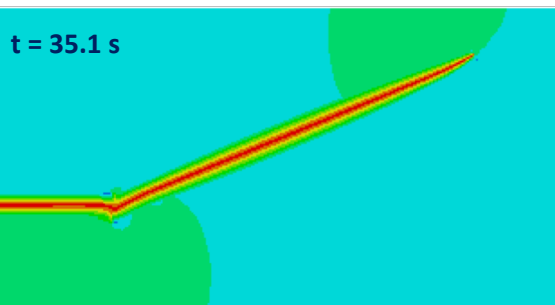
The sketch is not to scale !



Property	Value
Rock mass	
Young's modulus	$E = 30 \text{ GPa}$
Poisson's ratio	$\nu = 0.22$
Biot's coefficient	$b = 1.0$
Porosity	$\varphi = 0.01$
Hydraulic conductivity	$k = 1.1 \times 10^{-16} \text{ m}^2$
Cohesive material (HF1, HF2)	
Tensile strength	$R_T = 2.0 \text{ MPa}$
Mode I fracture energy	$G_{IC} = 62 \text{ N/m}$ $(K_{IC} = 1.4 \text{ MPa.m}^{0.5})$
Cohesive material fault F1	
Hydraulic aperture	0.4 mm
Friction coefficient	$\mu_f = 0.35$
Fracturing and pore fluid	
Dynamic viscosity	$\eta = 0.001 \text{ Pa}$
Density	$\rho = 1000 \text{ kg/m}^3$
Initial conditions	
Initial stresses	$S_h = 29, S_v = 36 \text{ MPa}$
Initial pore pressure	$p_0 = 23.7 \text{ MPa}$
Injection rate	$Q = 0.5 \text{ L/s per unit thickness}$

Pore pressures at different times

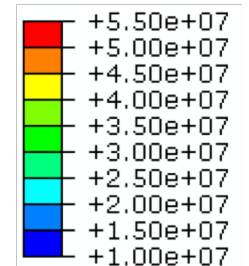
Case with $\mu_f = 0.35$, $Q = 0.5 \text{ L/s}$, and $\theta = 22^\circ$



The hydraulic fracture HF1 is generated and extends

HF1 intersects the fault F1 after 35.1 s of injection

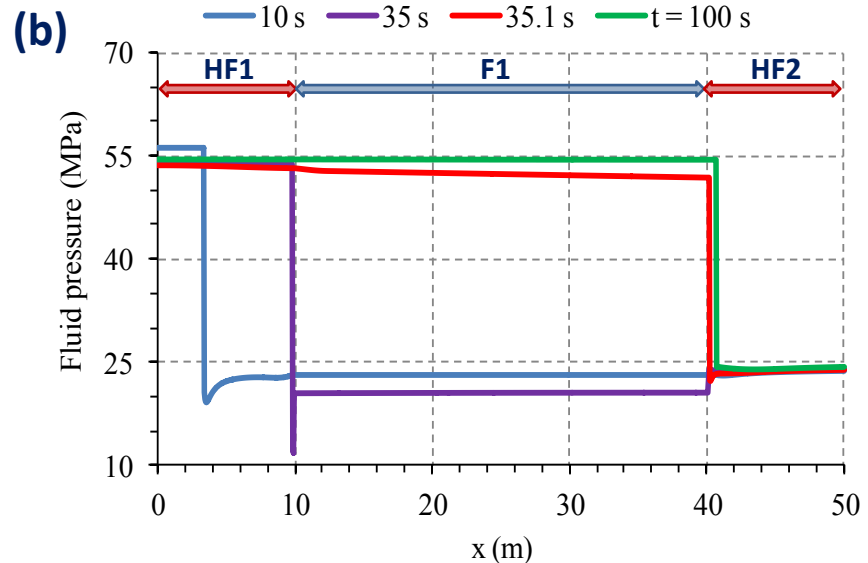
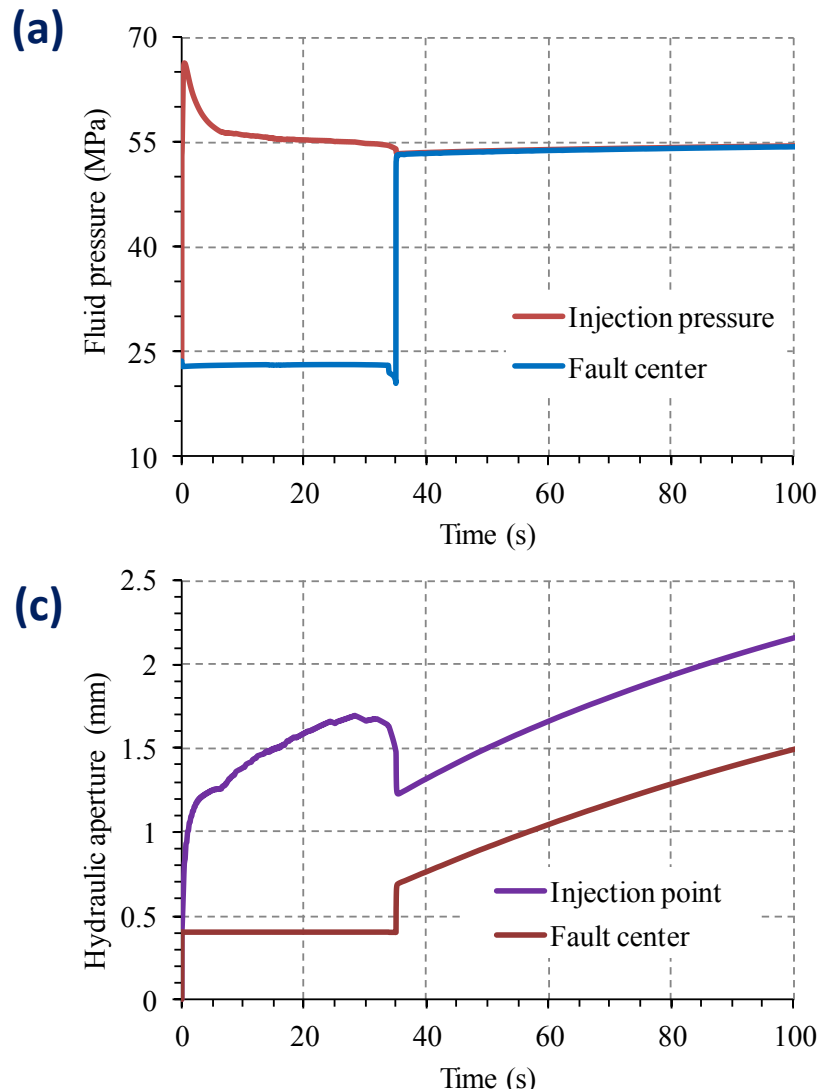
Pore pressure (Pa)



The hydraulic fracture HF2 is initiated

Time evolution of pressures and hydraulic apertures

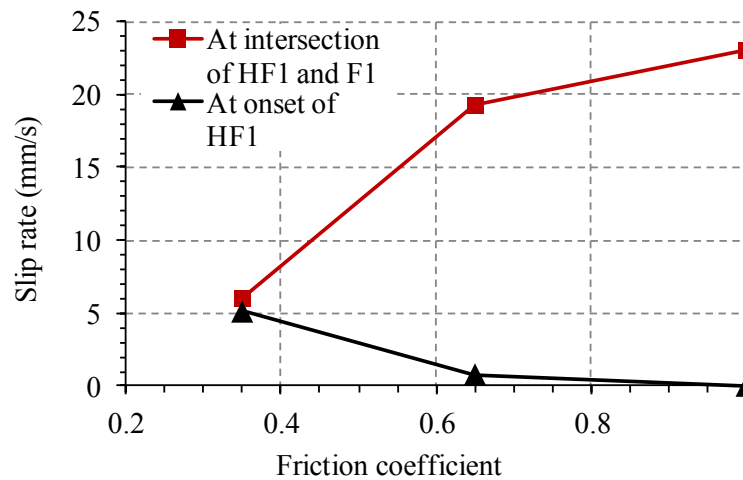
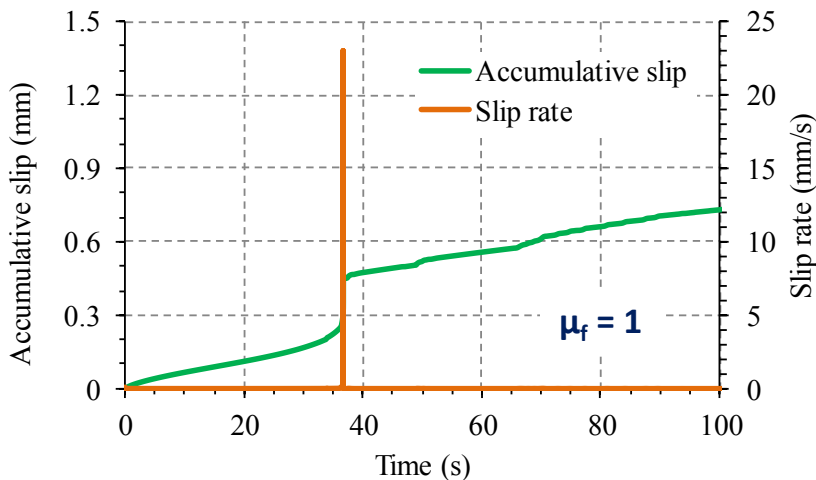
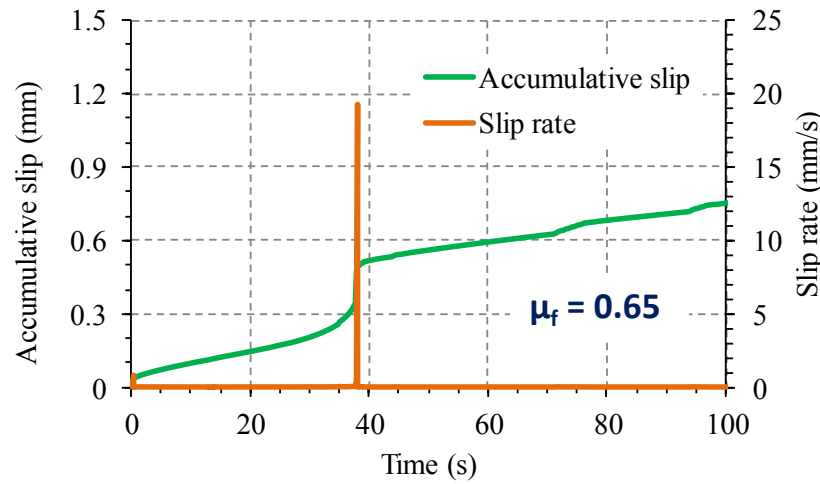
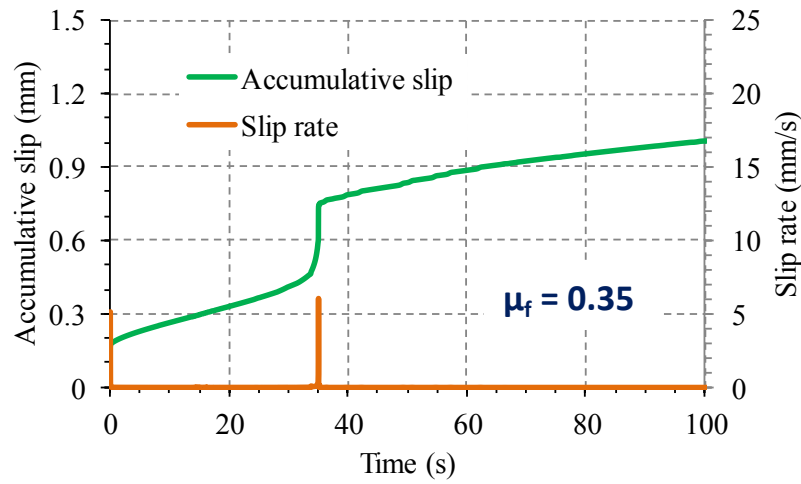
Case with $\mu_f = 0.35$, $Q = 0.5 \text{ L/s}$, and $\theta = 22^\circ$



- (a) Injection pressure (BHP) and fluid pressure at the center of the fault F1
- (b) Hydraulic aperture at injection point and at the center of the fault F1
- (c) Distribution of fluid pressure along path that consists of fracture HF1, fault F1, and fracture HF2 at different times

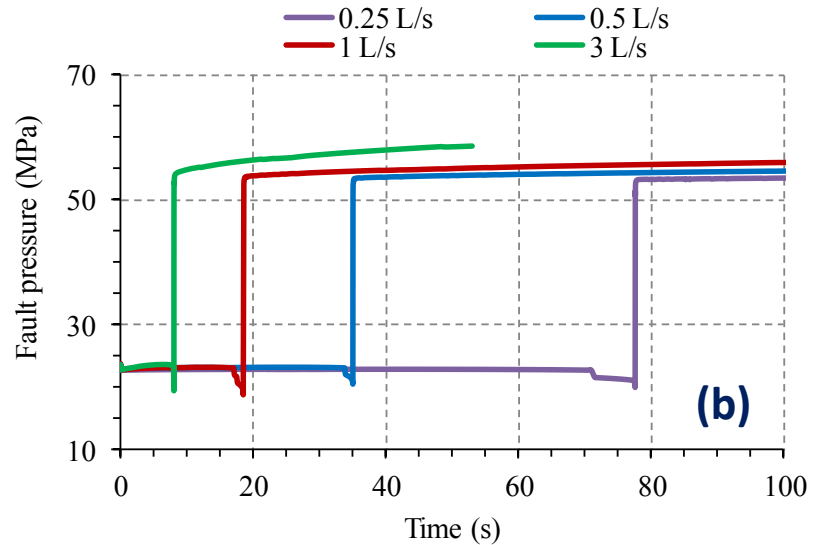
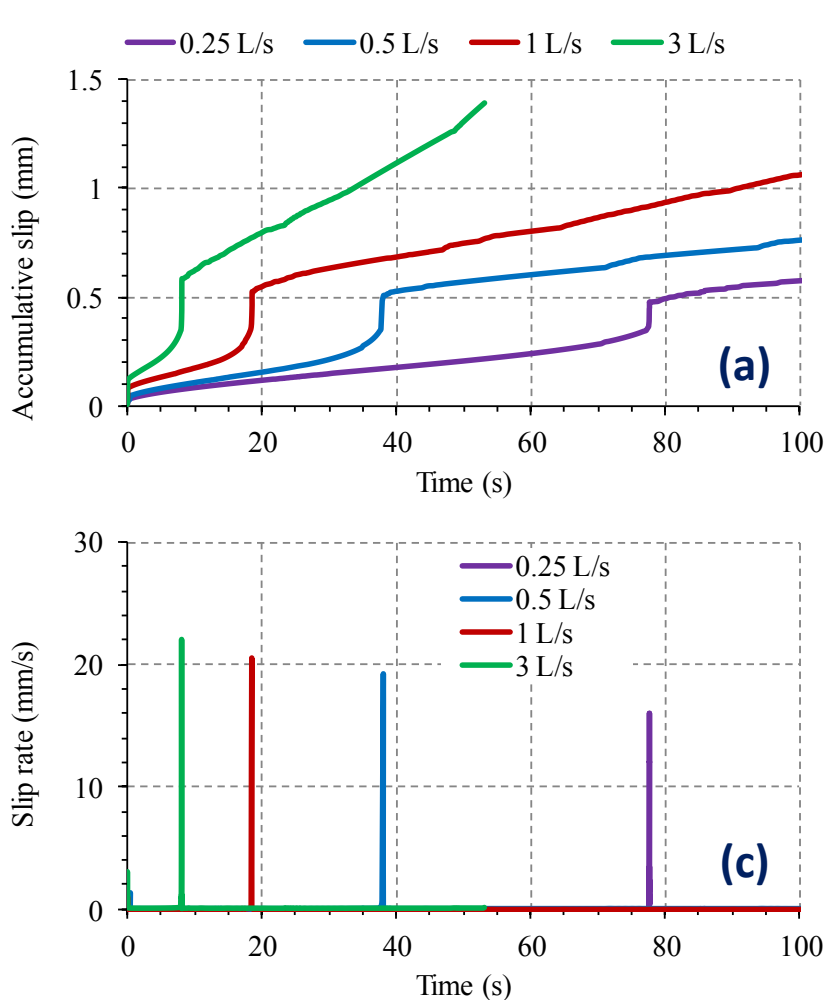
Average total slip and average slip rate of the fault F1

Effect of friction coefficient
($Q = 0.5 \text{ L/s}$ and $\theta = 22^\circ$)



Average total slip and average slip rate of the fault F1

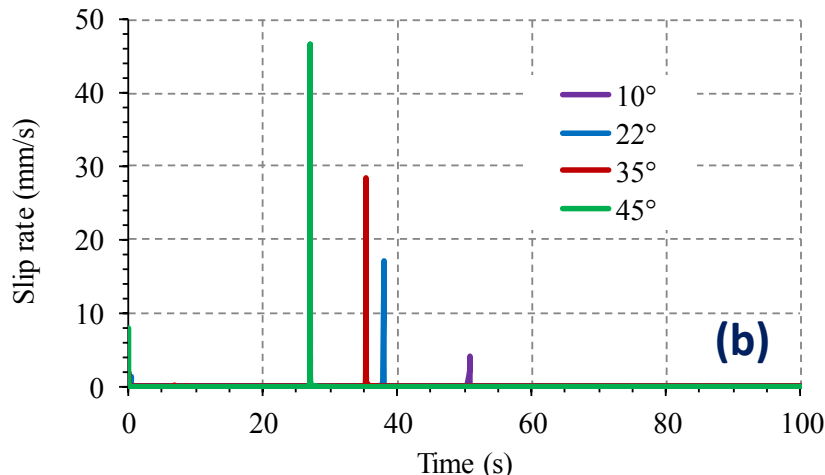
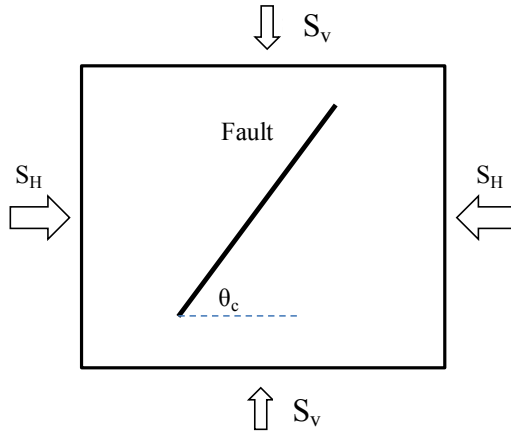
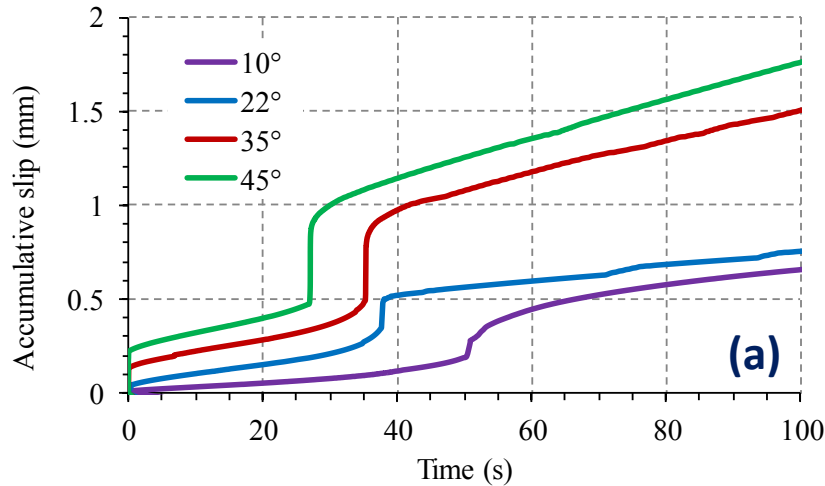
Effect of injection rate
($\mu_f = 0.35$ and $\theta = 22^\circ$)



- (a) Injection pressure (BHP) and fluid pressure at the center of the fault F1
- (b) Distribution of fluid pressure along path that consists of fracture HF1, fault F1, and fracture HF2 at different times
- (c) Slip rate of the fault F1

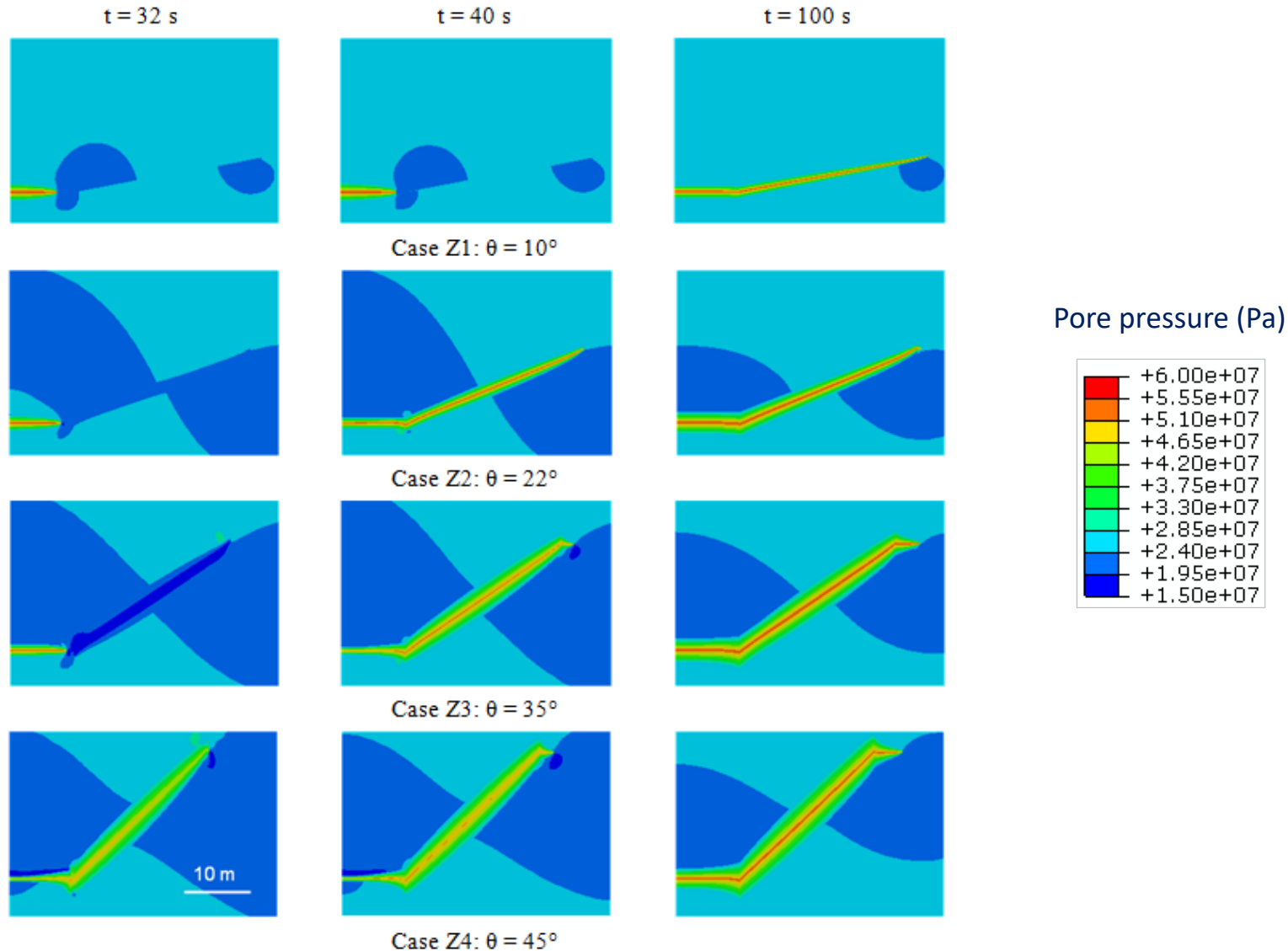
Average total slip and average slip rate of the fault F1

Effect of fault orientation
($\mu_f = 0.65$, $Q = 0.5$ L/s)



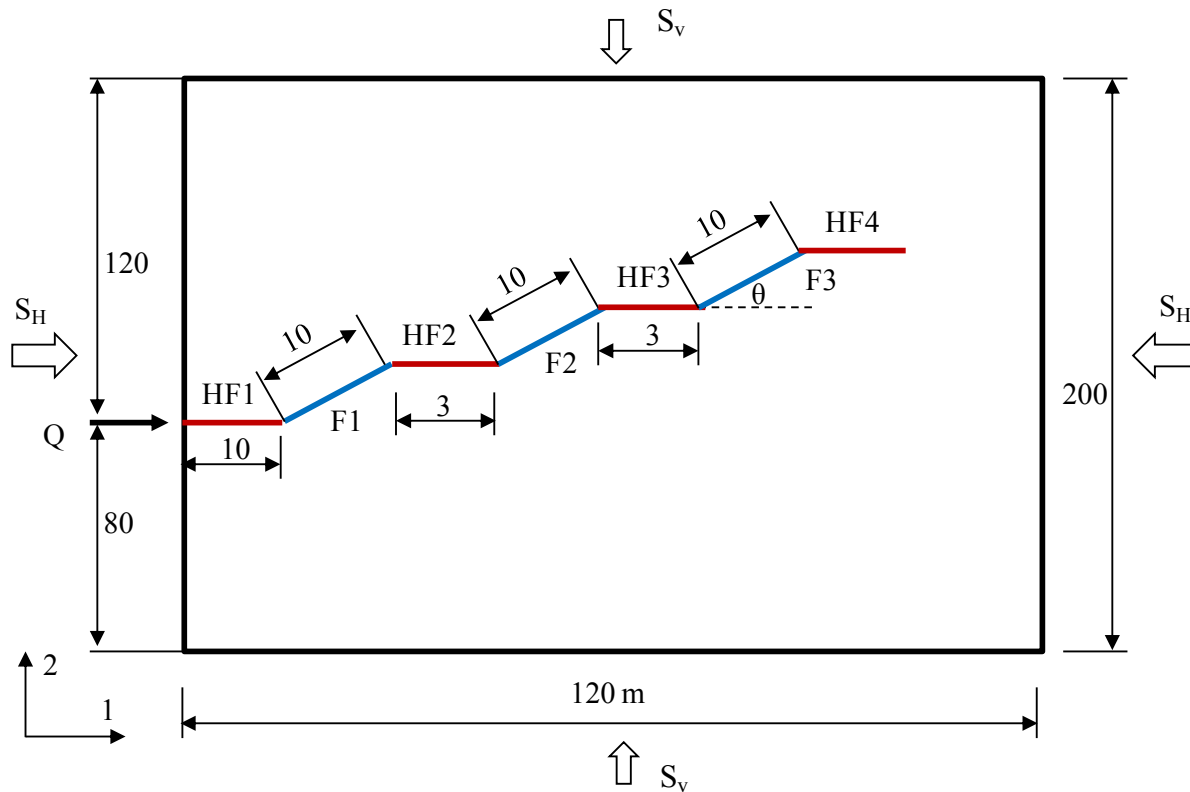
- (a) Accumulative slip as a function of time
(b) Slip rate of the fault F1 with different fault orientation angle from 10° to 45°

Pore pressure distribution at different times for different fault orientation



Slip induced by interaction of hydraulic fractures with multiple faults

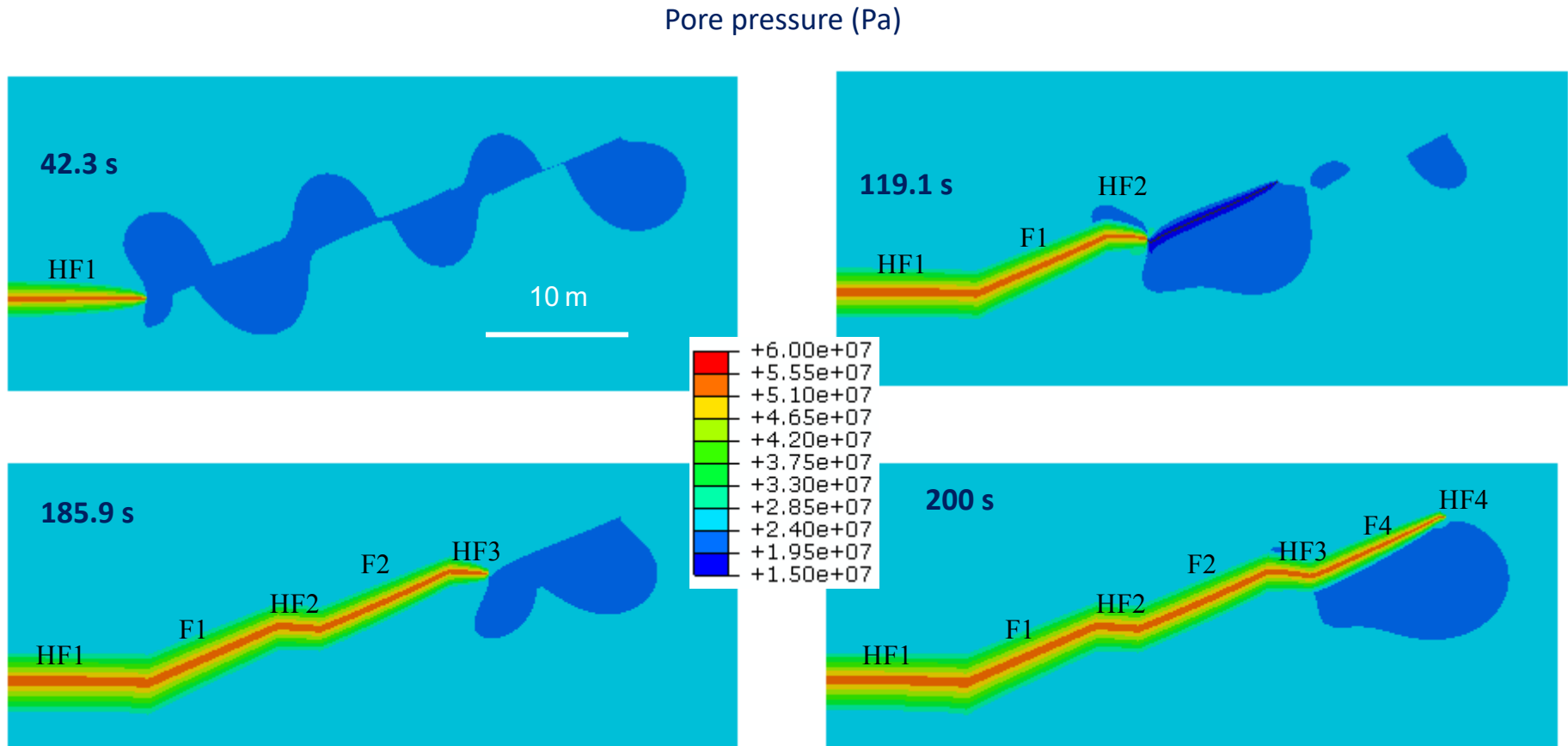
The sketch is not to scale !



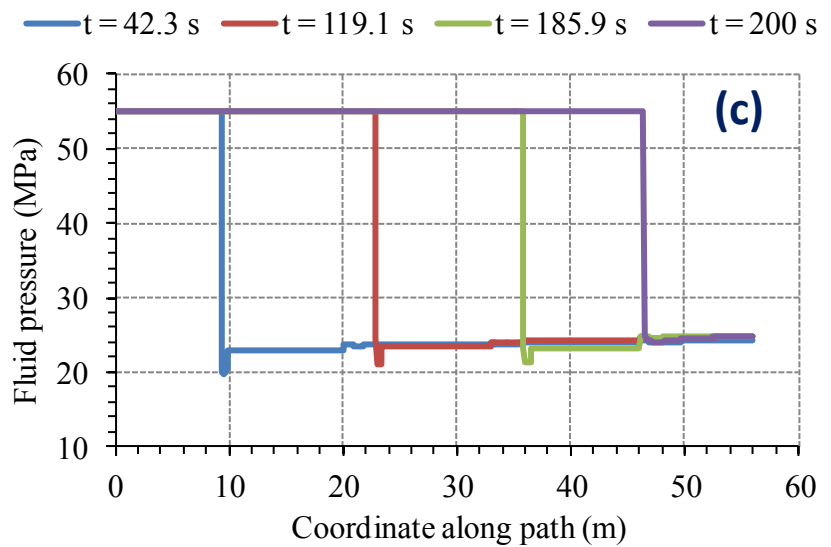
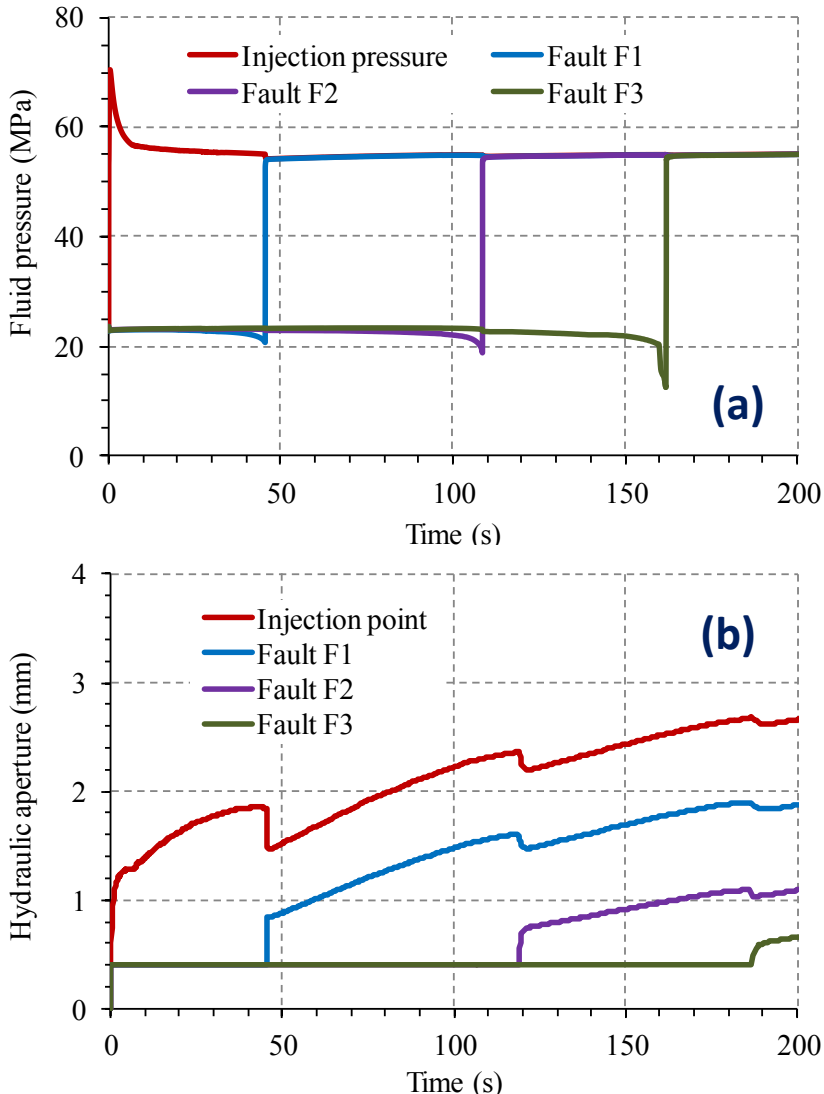
- 3 existing faults F1, F2 and F3, which are all oriented at 22° from the X direction
- Far-field stresses $S_H = 36 \text{ MPa}$ and $S_v = 29 \text{ MPa}$

Pore pressure at different times

Case 1 with $\mu = 0.35$; Injection rate = 0.5 L/s



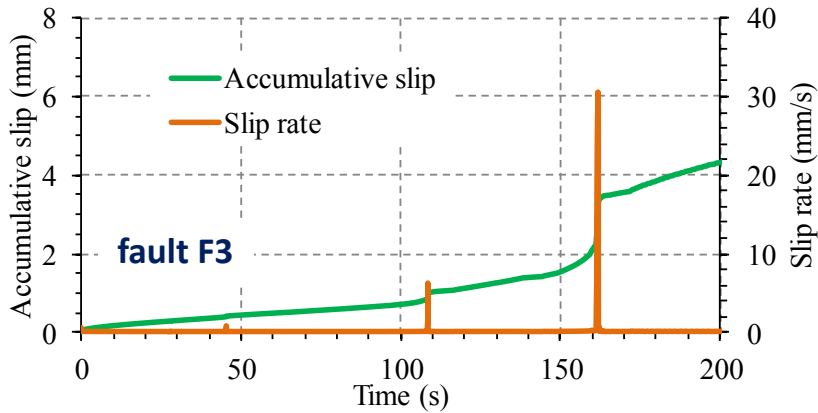
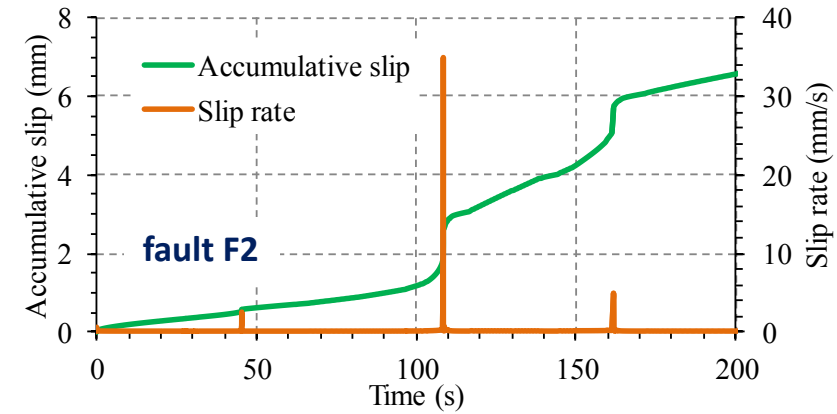
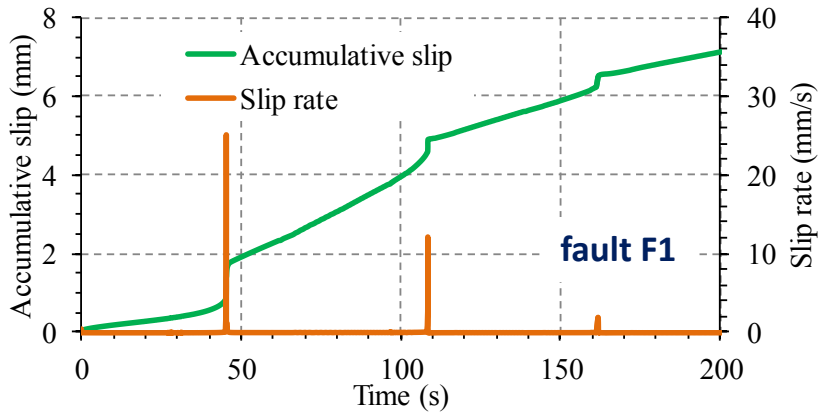
Time evolution of pressures and hydraulic apertures



Simulation results of case (friction coefficient $\mu_f = 0.65$): time evolution of

- (a) injection pressure and fluid pressure at the center of faults F1, F2, F3
- (b) hydraulic aperture at injection point and at the center of faults F1, F2, F3
- (c) Distribution of fluid pressure along path that consists of fracture HF1, fault F1, and fracture HF2 at different times

Average total slip and average slip rate of the faults

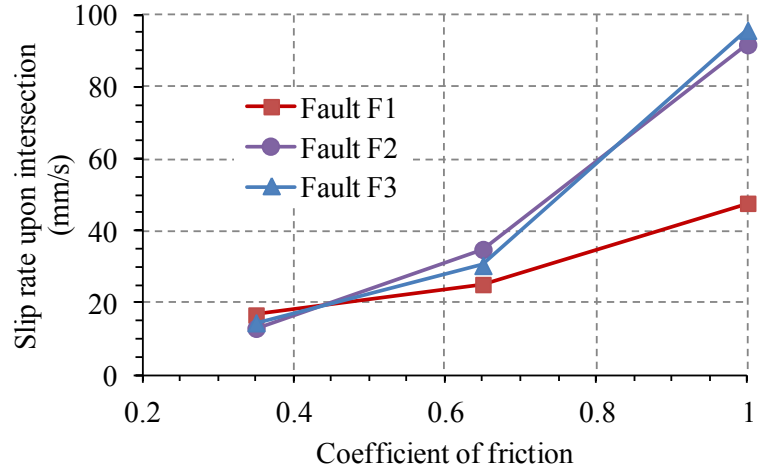
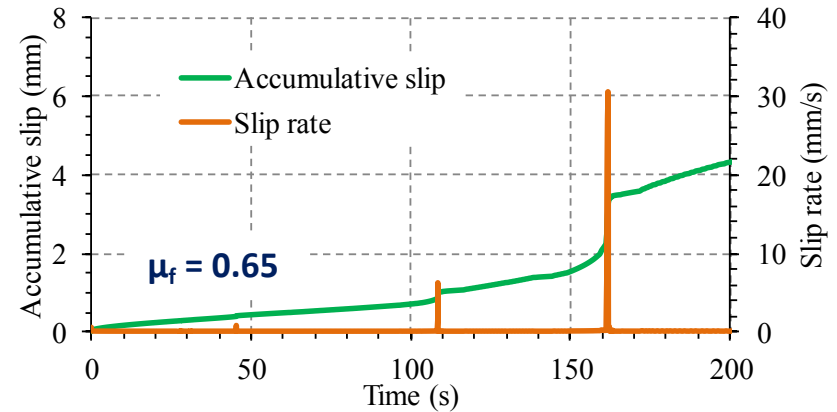
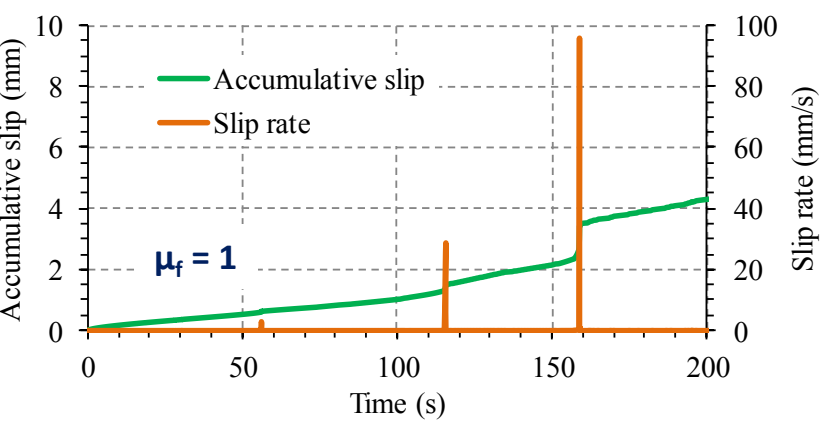
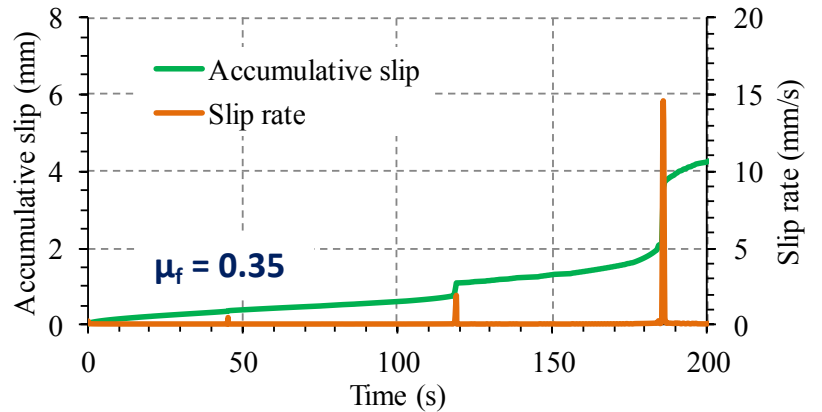


Simulation results of case MS2

$$\mu_f = 0.65, Q = 0.5 \text{ L/s}$$

Average total slip and average slip rate of the fault F3

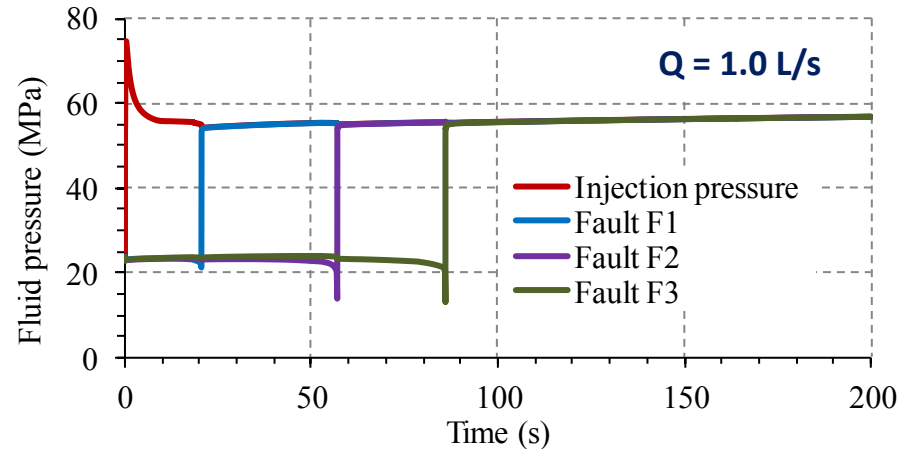
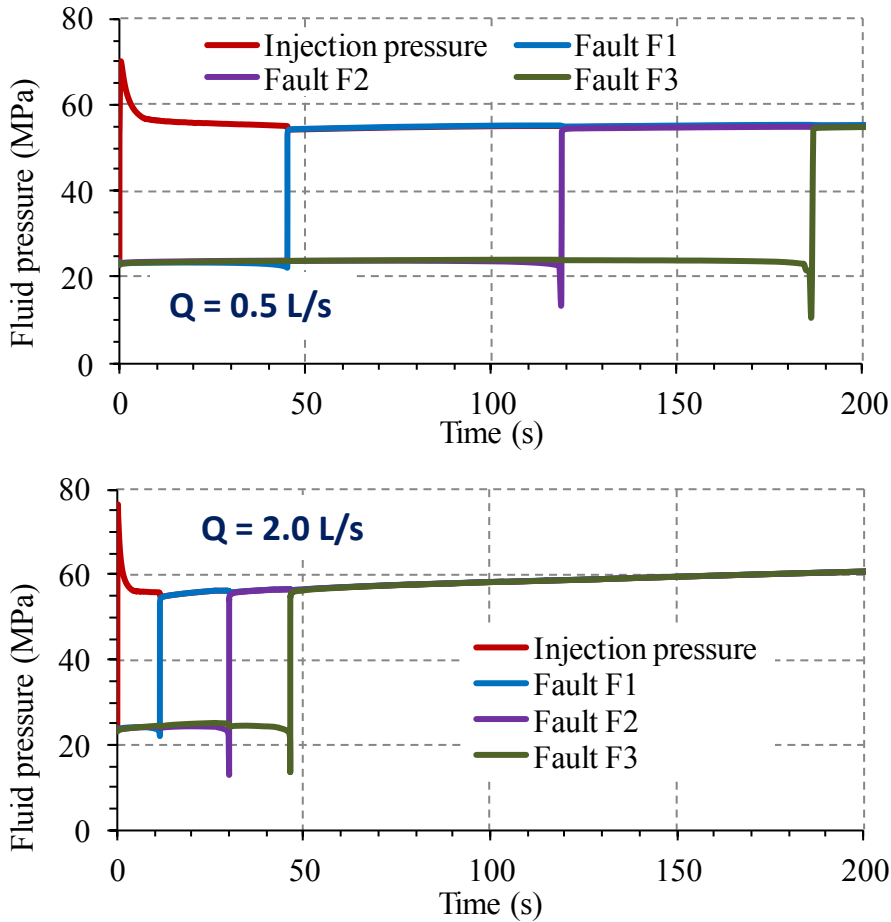
Effect of friction coefficient



Maximum slip rate upon intersection
as function of friction coefficient

Time evolution of injection pressure and fluid pressure at the center of faults F1, F2, F3

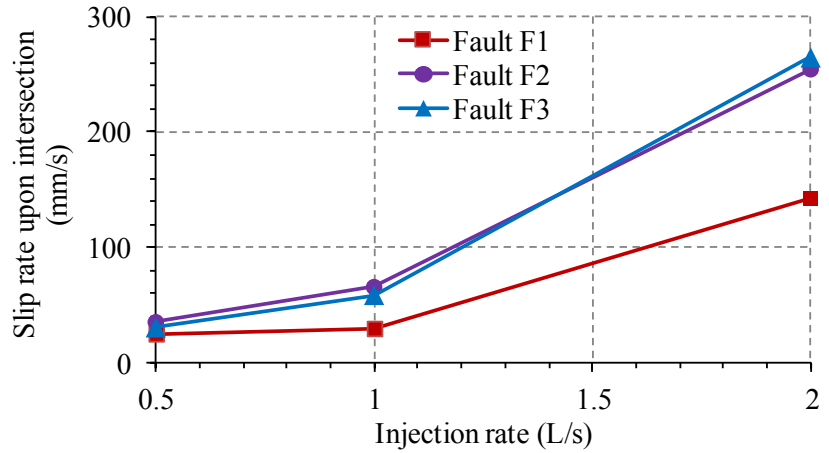
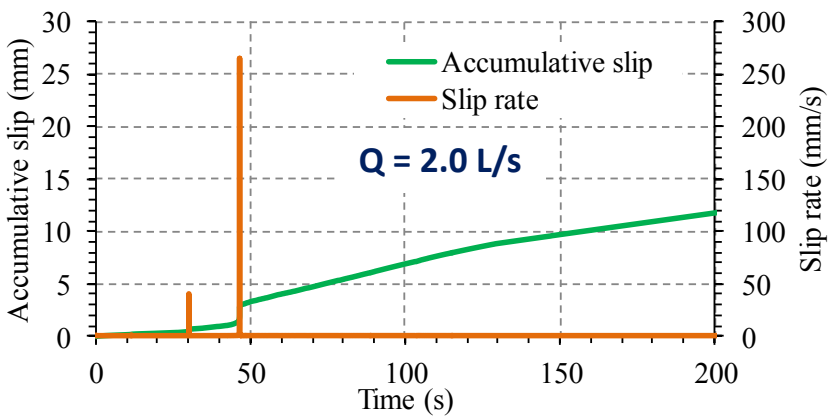
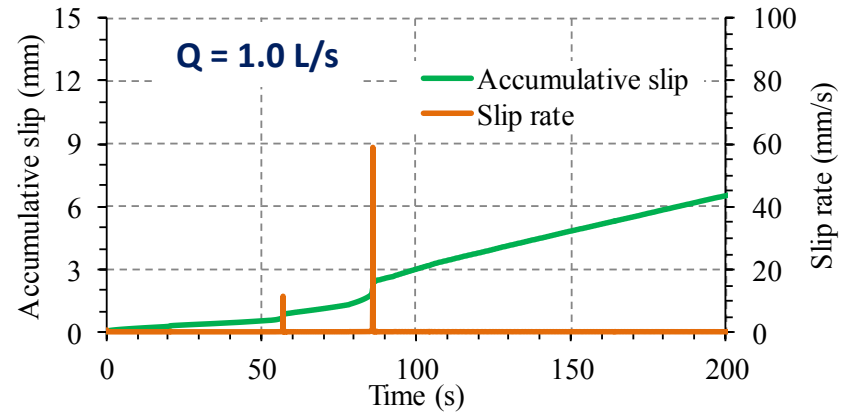
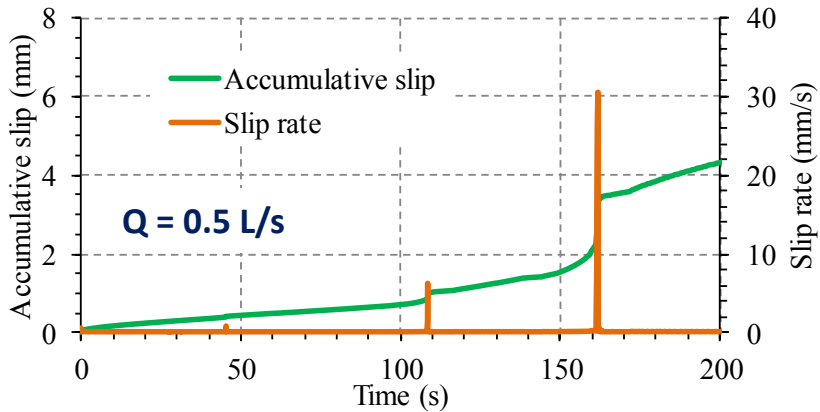
Effect of injection rate



The moment when the pressure in a fault suddenly increases corresponds the moment of intersection of the fault with a hydraulic fracture.

Average total slip and average slip rate of the fault F3

Effect of injection rate



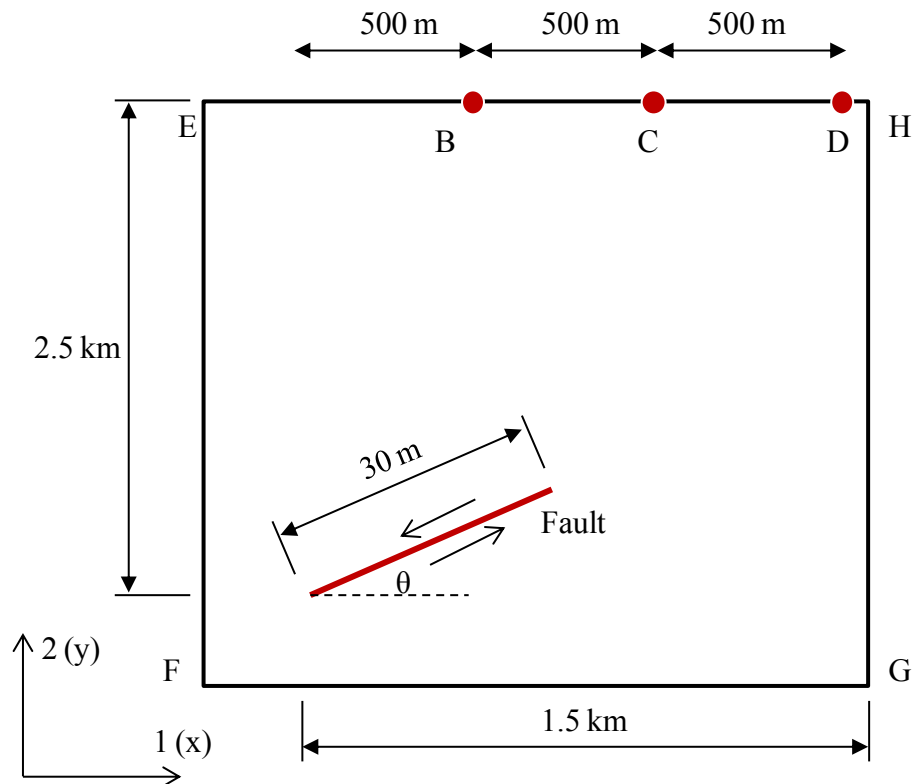
Slip rate of faults upon their intersection
with hydraulic fractures

Simulation of induced dynamic effects and wave propagation

Induced dynamic effects and wave propagation

Model for dynamic simulation

The sketch is not to scale !



2D Dynamic FEA (Abaqus)

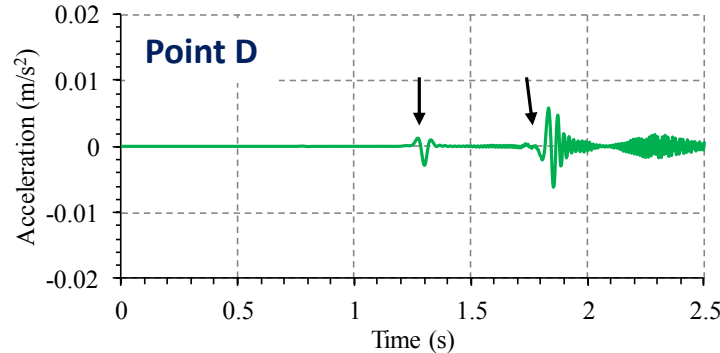
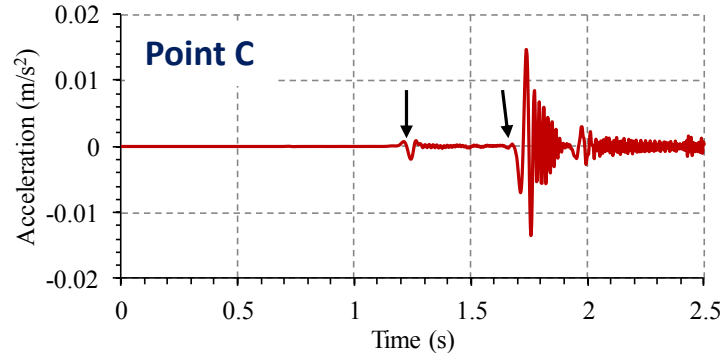
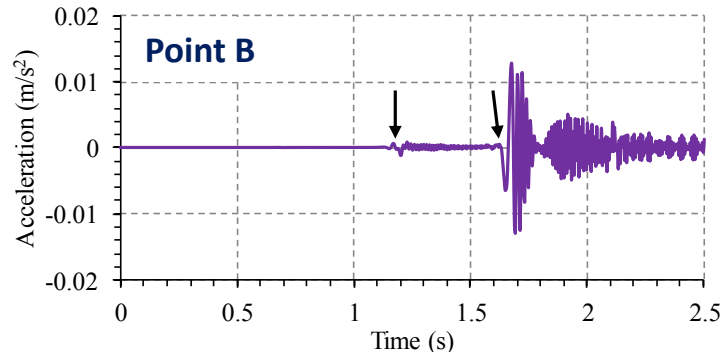
Property	Value
Undrained Young's modulus	$E_u = 36.9 \text{ GPa}$
Undrained Poisson's ratio	$\nu_u = 0.5$
Dilatational wave speed	$C_p = 3767 \text{ m/s}$
Shear wave speed	$C_s = 2174 \text{ m/s}$
Saturated density	$\rho = 2600 \text{ kg/m}^3$

Loading : the time history of fault displacements

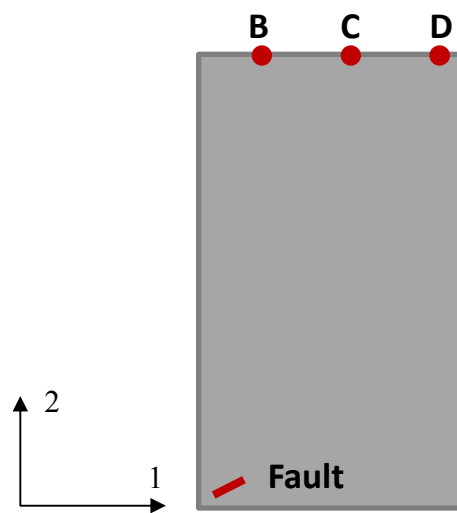
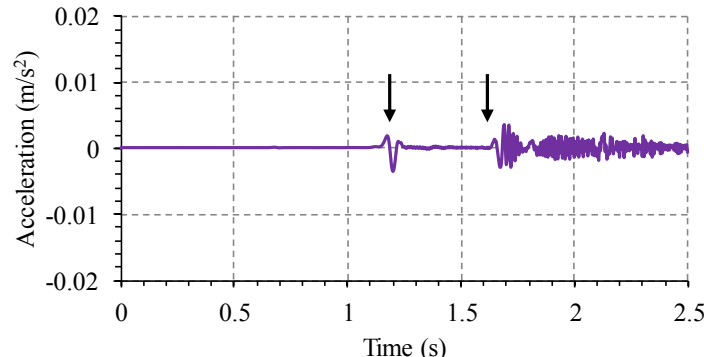
Quiet Boundary Conditions

Time evolution of acceleration at points B, C, and D

in direction 1



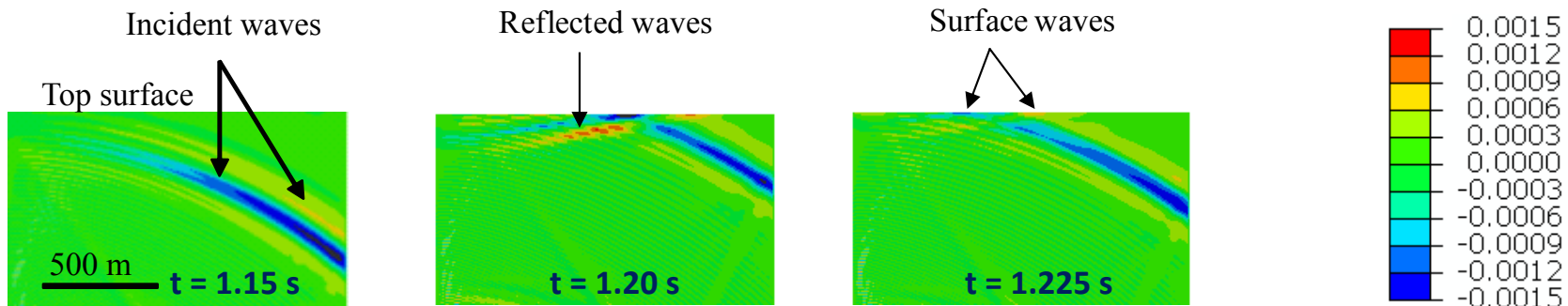
in direction 2



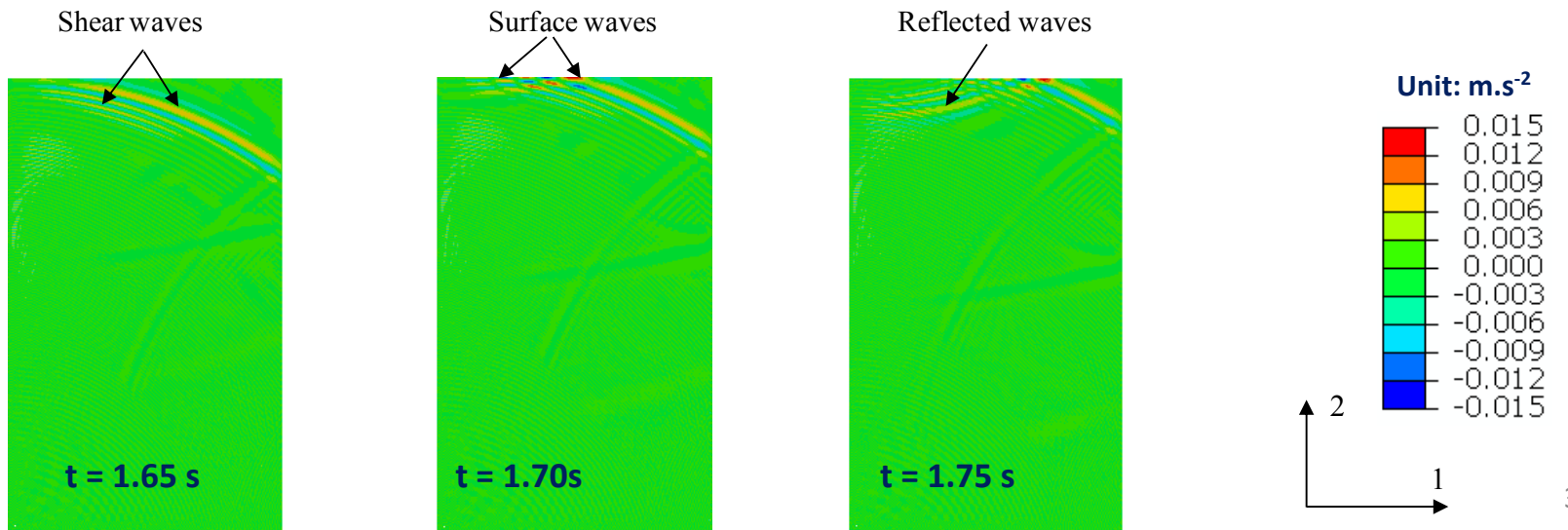
Arrows indicate the arrivals of elastic waves: left arrow for P waves; right arrow for S waves

Acceleration in direction 1 at different times

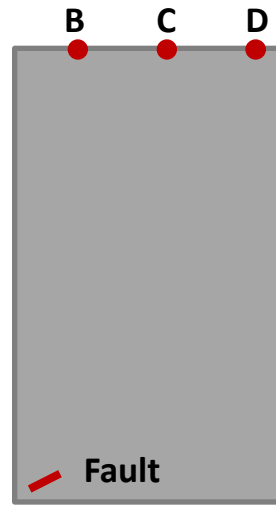
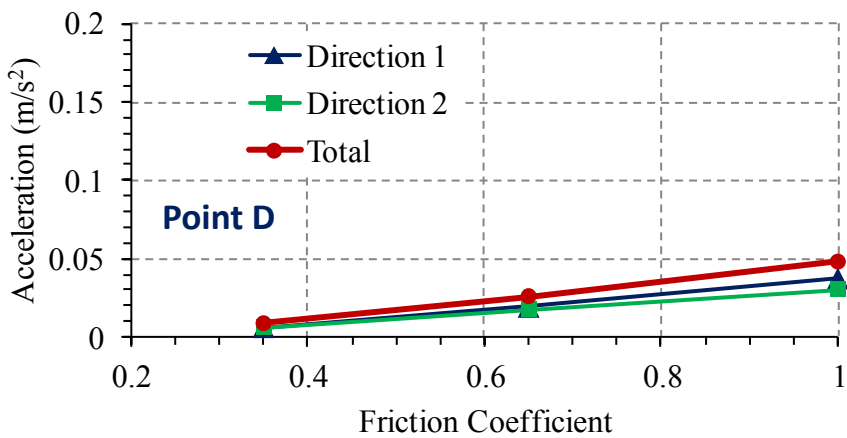
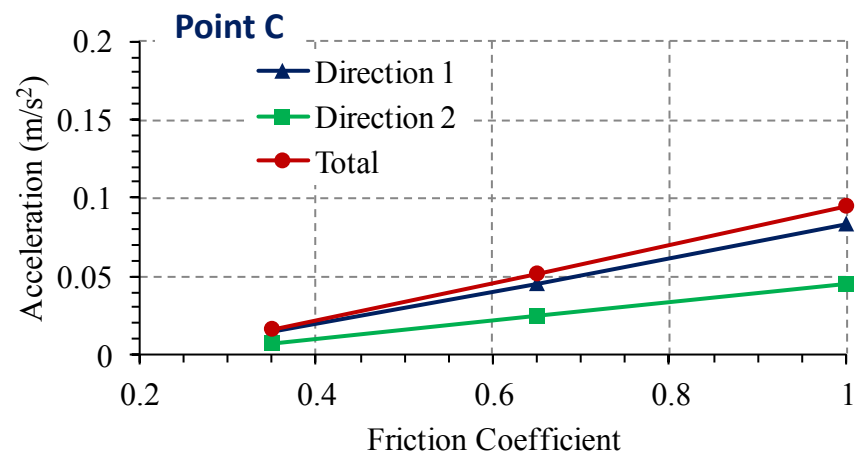
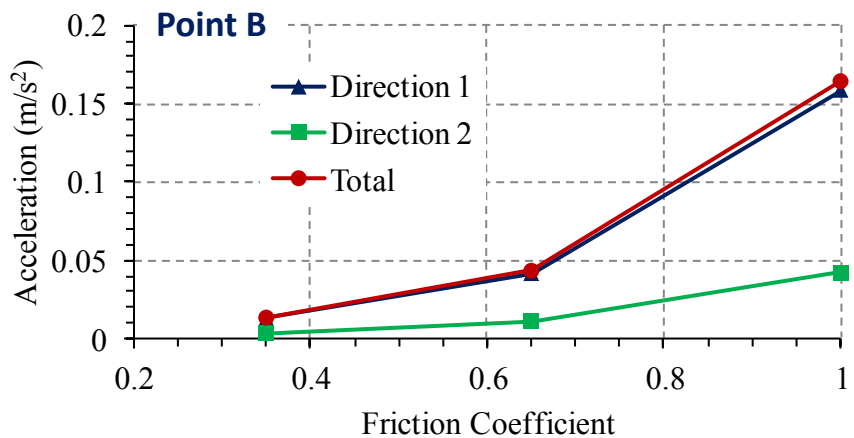
- Arrival of P waves to the top surface and generation of surface waves (Only the upper part of the model is presented)



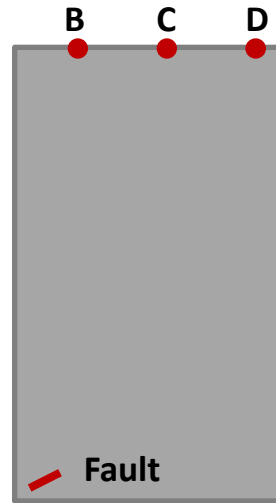
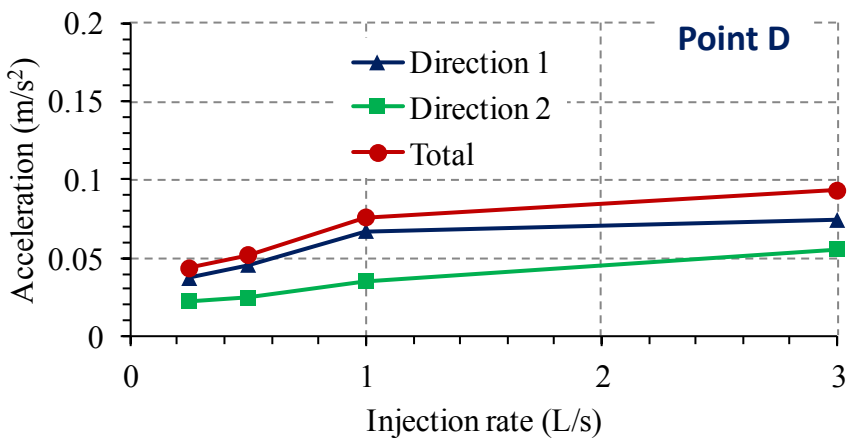
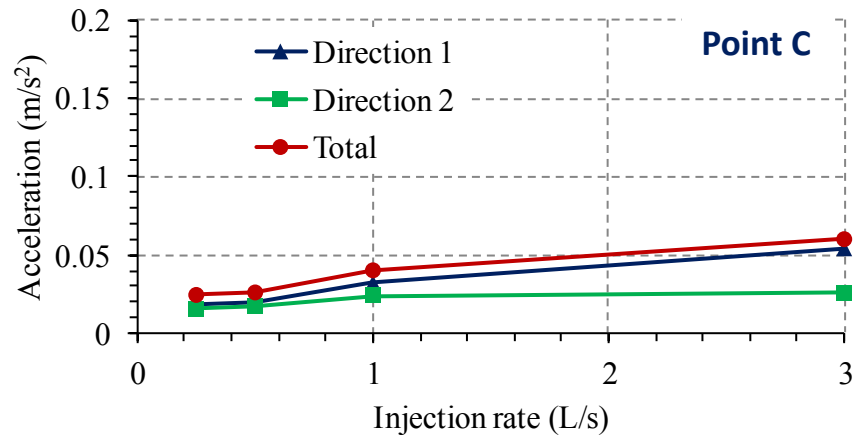
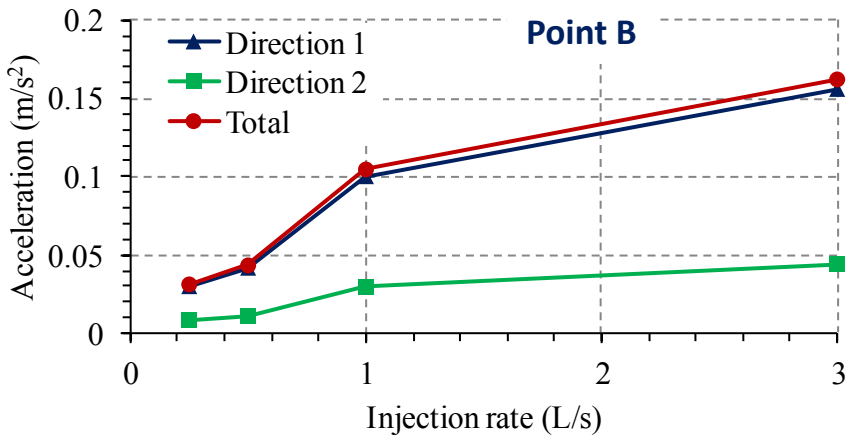
- Arrival of S waves to the top surface and generation of surface waves (The whole model is presented)



Peak Ground Acceleration at points B, C, and D as function of friction coefficient



Peak Ground Acceleration at points B, C, and D as function of injection rate



Summary and Conclusion

- A methodology has been developed to model induced seismicity during the hydraulic stimulation of deep geothermal reservoir.

Intensity	Peak acceleration (% g)	Peak velocity (cm/s)	Perceived shaking	Potential damage
I	< 0.17	< 0.1	Not felt	None
II–III	0.17–1.4	0.1–1.1	Weak	None
IV	1.4–3.9	1.1–3.4	Light	None

- It is found that both the friction coefficient of existing faults and the rate of injection play a major role on the fault slip rates and eventually on the Peak Ground Acceleration and Velocity (Smooth Stimulation)

Next:

- Extrapolation to geothermal reservoir with real DFN with accounting for uncertainties

Merci de votre attention !